

VASP6: total energies beyond DFT

Martijn Marsman

University Vienna & VASP Software GmbH



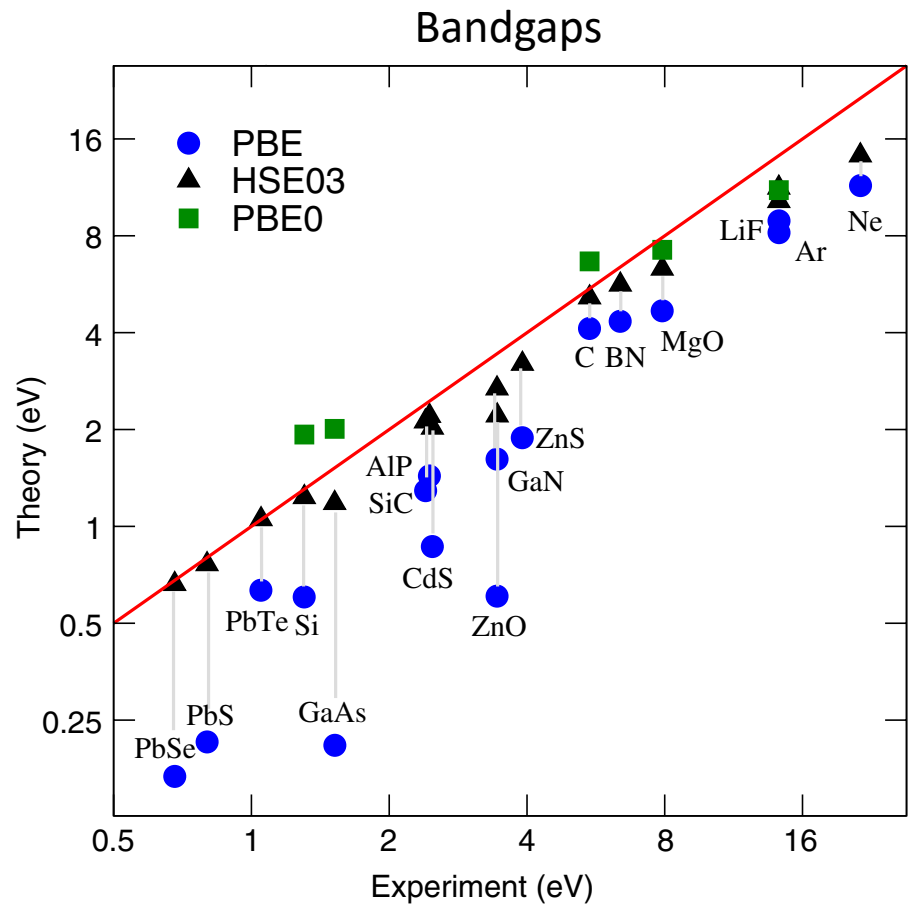
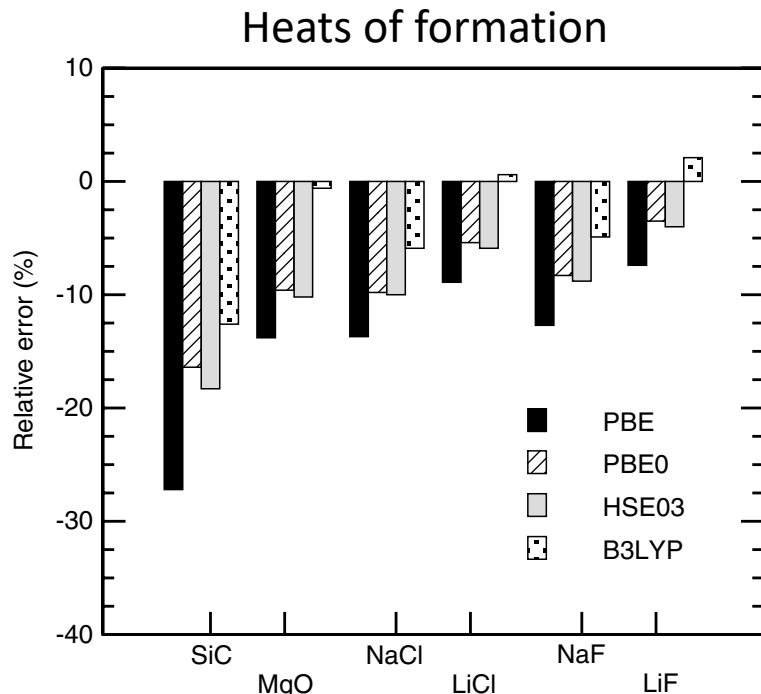
universität
wien

b-initio
VAsP package
ienna simulation

Outline

- Beyond DFT
 - The need to go beyond DFT
 - HF/DFT hybrid functionals
 - The Random-Phase-Approximation
- $O(N^3)$ implementation of the RPA
 - Cubic-scaling RPA total energies
 - Minimax frequency and time integration
 - Cubic-scaling RPA quasi-particles
- Forces in the RPA

Need to go beyond DFT and DFT/HF hybrids?



- Total energy differences with “chemical accuracy” (1 kcal/mol \approx 40 meV/atom): Atomization-, formation energies, reaction barriers, etc
- Van der Waals interactions

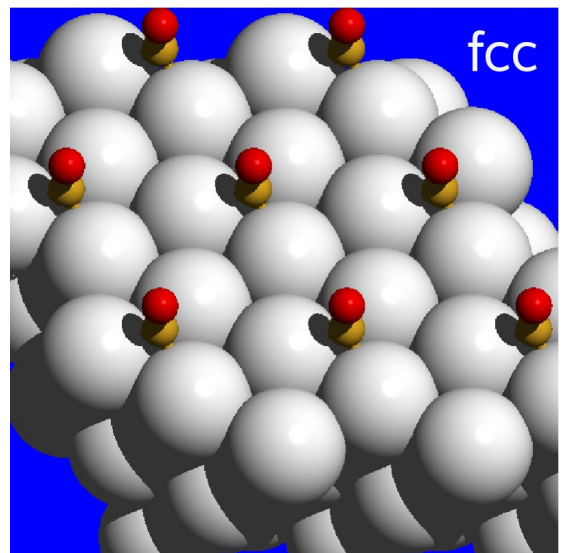
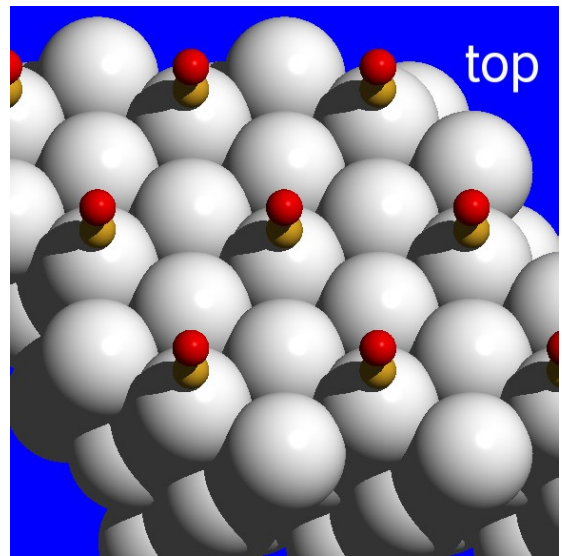
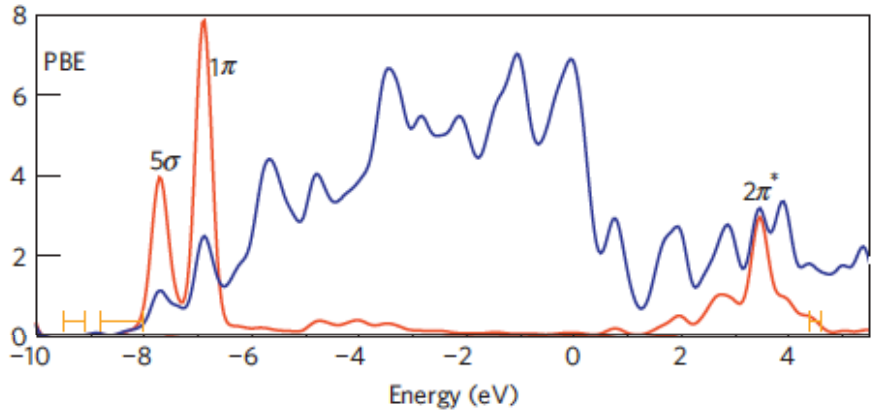
- Bandstructure of metals and *largish* gap systems, and some problematic cases inbetween

CO adsorption on d-metal surfaces

- DFT incorrectly predicts that CO prefers the hollow site: P. Feibelman *et al.*, J. Phys. Chem. B 105, 4018 (2001)
- This error is relatively large.
Best DFT/PBE calculations:

CO@Cu(111): -170 meV
CO@Rh(111): -40 meV
CO@Pt(111): -100 meV

- CO HOMO-LUMO gap too small in DFT:



CO adsorption on d-metal surfaces

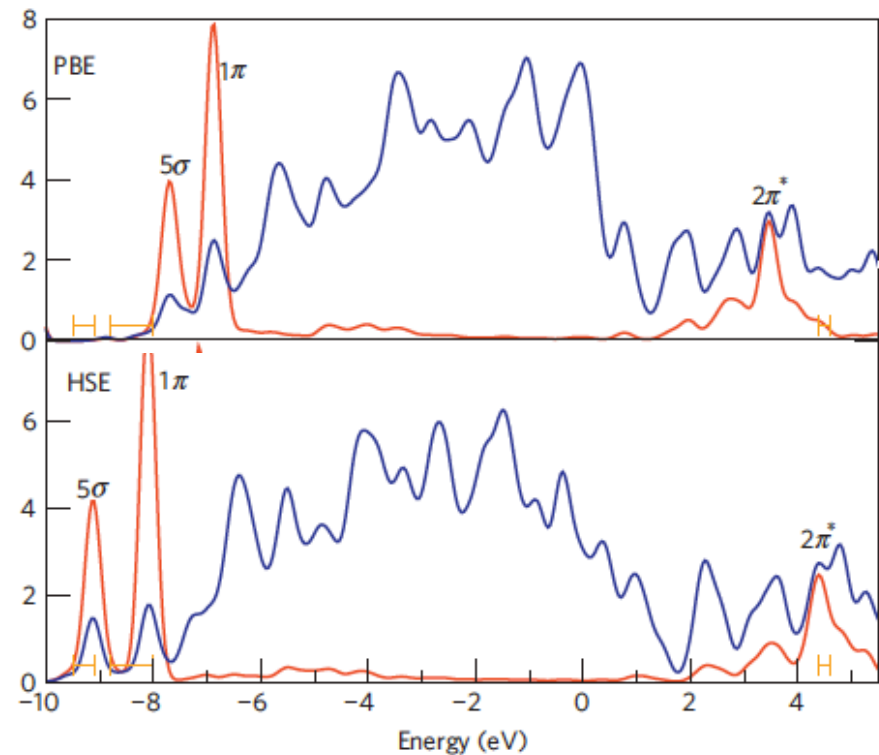
CO @		top	fcc	hcp	Δ
Cu(111)	PBE	0.709	0.874	0.862	-0.165
	PBE0	0.606	0.579	0.565	0.027
	HSE03	0.561	0.555	0.535	0.006
	exp.	0.46-0.52			
Rh(111)	PBE	1.870	1.906	1.969	-0.099
	PBE0	2.109	2.024	2.104	0.005
	HSE03	2.012	1.913	1.996	0.016
	exp.	1.43-1.65			
Pt(111)	PBE	1.659	1.816	1.750	-0.157
	PBE0	1.941	1.997	1.944	-0.056
	HSE03	1.793	1.862	1.808	-0.069
	exp.	1.43-1.71			

(All energies in eV)

Hybrid functionals reduce the tendency to stabilize adsorption at the hollow site w.r.t. the top site.

reduced CO $2\pi^*$ – metal-*d* interaction

- DFT does well for the metallic surface, but not for the CO: $2\pi^*$ (LUMO) too close to the Fermi level.
- HSE does well for the CO, but not for the surface: *d*-metal bandwidth too large.



Schimka et al., Nature Materials 9, 741 (2010)

The Random-Phase-Approximation: GW and ACFDT

- Quasiparticles from GW: “electronic structure” in the RPA.
- Total energies from the ACFDT in the RPA.
- Are the above related?

One-electron/QP picture

DFT: Kohn-Sham eq.

$$\left(-\frac{1}{2}\Delta + V_{\text{ext}}(\mathbf{r}) + V_{\text{H}}(\mathbf{r}) + V_{\text{xc}}[\rho](\mathbf{r}) \right) \psi_{n\mathbf{k}}(\mathbf{r}) = \epsilon_{n\mathbf{k}} \psi_{n\mathbf{k}}(\mathbf{r})$$

DFT-HF hybrid functionals: Roothaan eq.

$$\left(-\frac{1}{2}\Delta + V_{\text{ext}}(\mathbf{r}) + V_{\text{H}}(\mathbf{r}) \right) \psi_{n\mathbf{k}}(\mathbf{r}) + \int V_{\text{X}}[\{\psi_o\}](\mathbf{r}, \mathbf{r}') \psi_{n\mathbf{k}}(\mathbf{r}') d\mathbf{r}' = \epsilon_{n\mathbf{k}} \psi_{n\mathbf{k}}(\mathbf{r})$$

GW: quasi-particle eq.

$$\left(-\frac{1}{2}\Delta + V_{\text{ext}}(\mathbf{r}) + V_{\text{H}}(\mathbf{r}) \right) \psi_{n\mathbf{k}}(\mathbf{r}) + \int \Sigma[\{\psi, E\}](\mathbf{r}, \mathbf{r}', E_{n\mathbf{k}}) \psi_{n\mathbf{k}}(\mathbf{r}') d\mathbf{r}' = E_{n\mathbf{k}} \psi_{n\mathbf{k}}(\mathbf{r})$$

GW

The quasi-particle equation:

$$\left(-\frac{1}{2}\Delta + V_{\text{ext}}(\mathbf{r}) + V_{\text{H}}(\mathbf{r}) \right) \psi_{n\mathbf{k}}(\mathbf{r}) + \int \Sigma(\mathbf{r}, \mathbf{r}', E_{n\mathbf{k}}) \psi_{n\mathbf{k}}(\mathbf{r}') d\mathbf{r}' = E_{n\mathbf{k}} \psi_{n\mathbf{k}}(\mathbf{r})$$

The “self-energy is given by:

$$\Sigma = iGW$$

or more explicitly

$$\Sigma(\mathbf{r}, \mathbf{r}', E) = \frac{i}{2\pi} \int_{-\infty}^{\infty} d\omega \sum_n^{\text{all}} \frac{\psi_n(\mathbf{r}) \psi_n^*(\mathbf{r}')}{\omega - E - E_n + i\eta \operatorname{sgn}(E_n - E_{\text{fermi}})} \times$$

$$\times e^2 \int d\mathbf{r}'' \frac{\epsilon^{-1}(\mathbf{r}, \mathbf{r}'', \omega)}{|\mathbf{r}'' - \mathbf{r}'|}$$

Green's function: G



screened Coulomb interaction: W

Compare to Fock-exchange:

$$V_X(\mathbf{r}, \mathbf{r}') = - \sum_n^{\text{occ.}} \psi_n(\mathbf{r}) \psi_n^*(\mathbf{r}') \times \frac{e^2}{|\mathbf{r} - \mathbf{r}'|}$$

bare Coulomb interaction: v

The Green's function: physical interpretation

The Green's function $G(\mathbf{r}, \mathbf{r}', t - t')$ describes the propagation of a particle from (\mathbf{r}, t) to (\mathbf{r}', t') : i.e., provided we have particle at position \mathbf{r} at time t , $G(\mathbf{r}, \mathbf{r}', t - t')$ is the chance of finding it at position \mathbf{r}' at time t' .

$$G_0(\mathbf{r}, \mathbf{r}', \omega) = \sum_n^{\text{all}} \frac{\psi_n^*(\mathbf{r})\psi_n(\mathbf{r}')}{\omega - \epsilon_n + i\eta \operatorname{sgn}(\epsilon_n - \mu)}$$

- Particle propagator: $G_o(1,2) = G_o(\mathbf{r}_1, \mathbf{r}_2, t_2 - t_1)$ for $t_2 > t_1$:

$$(\mathbf{r}_1, t_1) = 1 \quad (\mathbf{r}_2, t_2) = 2$$


$$G_0(1, 2) = \sum_n^{\text{vir.}} \psi_n(\mathbf{r}_1)^* \psi_n(\mathbf{r}_2) e^{-i(\epsilon_n - \mu)(t_2 - t_1)}$$

- Hole propagator: $G_o(1,2)$ for $t_1 > t_2$:

$$(\mathbf{r}_2, t_2) = 2 \quad (\mathbf{r}_1, t_1) = 1$$


$$G_0(1, 2) = \sum_n^{\text{occ.}} \psi_n^*(\mathbf{r}_1) \psi_n(\mathbf{r}_2) e^{-i(\epsilon_n - \mu)(t_1 - t_2)}$$

W in the Random-Phase-Approximation

Key: the “irreducible polarizability in the independent particle picture” χ^0 (or χ^{KS}):

$$\chi^0(\mathbf{r}, \mathbf{r}', \omega) := \frac{\partial \rho_{\text{ind}}(\mathbf{r}, \omega)}{\partial v_{\text{eff}}(\mathbf{r}', \omega)}$$

In the RPA, the screened Coulomb interaction is computed from χ^0 as:

$$W = \nu + \nu\chi_0\nu + \nu\chi_0\nu\chi_0\nu + \nu\chi_0\nu\chi_0\nu\chi_0\nu + \dots = \nu \underbrace{(1 - \chi_0\nu)^{-1}}_{\epsilon^{-1}}$$

geometrical series

and so on,
and so on ...

1. The bare Coulomb interaction between two particles

2. The electronic environment reacts to the field generated by a particle: induced change in the density $\chi_0\nu$, that gives rise to a change in the Hartree potential: $\nu\chi_0\nu$.

3. The electrons react to the induced change in the potential: additional change in the density, $\chi_0\nu\chi_0\nu$, and corresponding change in the Hartree potential: $\nu\chi_0\nu\chi_0\nu$.

$$W = \epsilon^{-1}\nu$$

$$\epsilon^{-1} = 1 + \nu\chi$$

$$\chi = \chi^0 + \chi^0\nu\chi$$

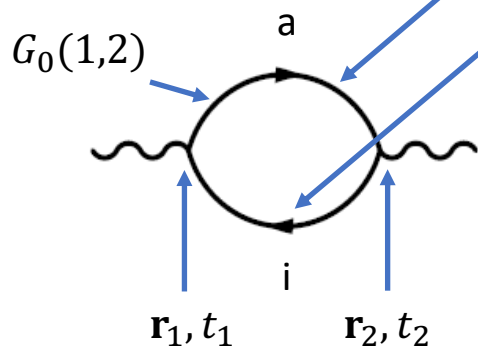
The IP-polarizability: χ_0

The “irreducible polarizability in the independent particle picture” χ^0 (or χ^{KS}):

$$\chi^0(\mathbf{r}, \mathbf{r}', \omega) := \frac{\partial \rho_{\text{ind}}(\mathbf{r}, \omega)}{\partial v_{\text{eff}}(\mathbf{r}', \omega)}$$

Adler and Wiser derived expressions for χ^0

$$\chi_0(\mathbf{r}_1, \mathbf{r}_2, \omega) = \sum_i^{\text{occ.}} \sum_a^{\text{virt.}} \frac{\langle \psi_a | \mathbf{r}_1 | \psi_i \rangle \langle \psi_i | \mathbf{r}_2 | \psi_a \rangle}{\epsilon_i - \epsilon_a - \omega} + \sum_i^{\text{occ.}} \sum_a^{\text{virt.}} \frac{\langle \psi_i | \mathbf{r}_1 | \psi_a \rangle \langle \psi_a | \mathbf{r}_2 | \psi_i \rangle}{\epsilon_a - \epsilon_i - \omega}$$

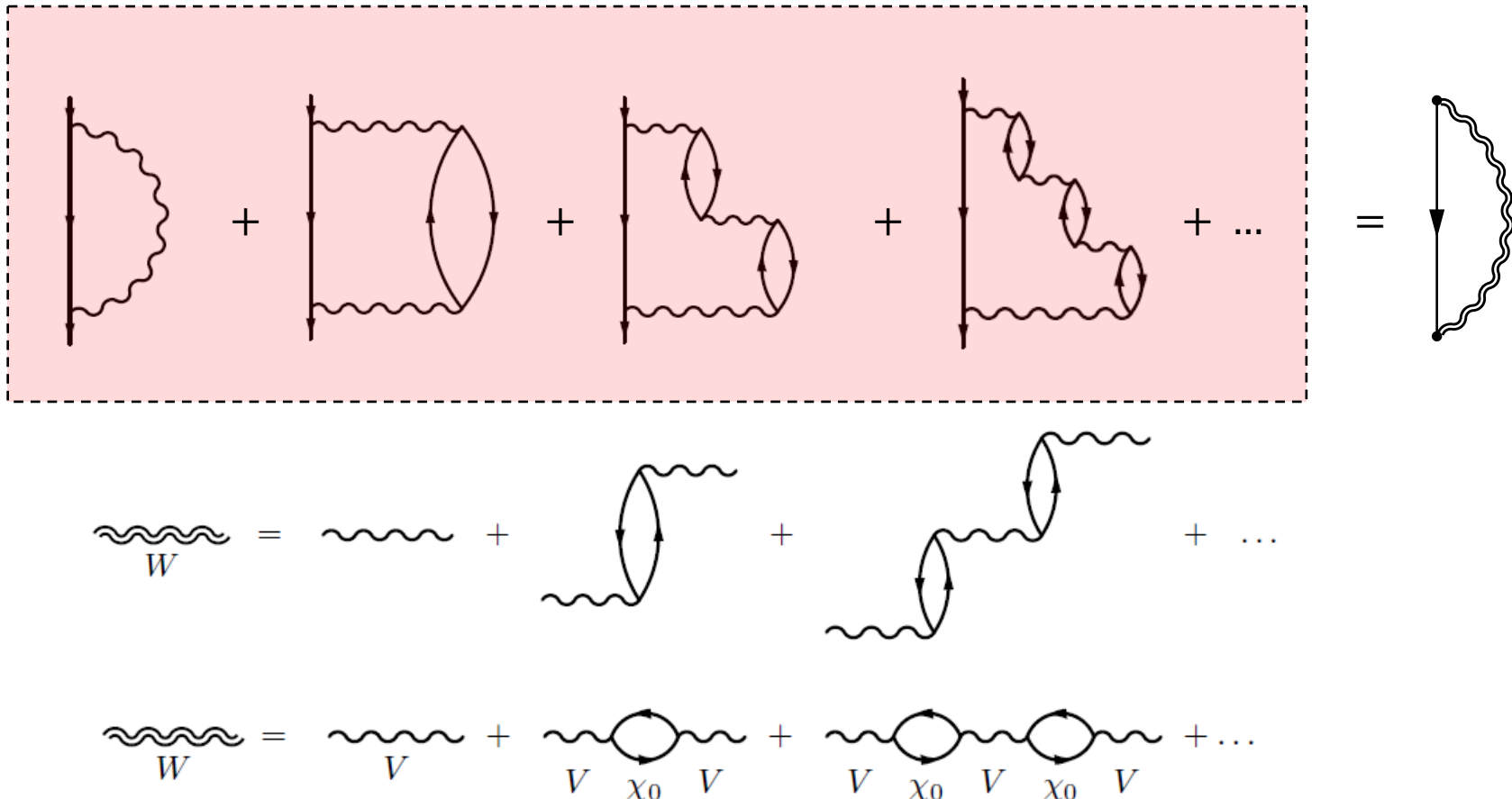


Or in terms of Green's functions (propagators):

$$\chi_0(\mathbf{r}_1, t_1, \mathbf{r}_2, t_2) = \chi(1, 2) = -G_0(1, 2)G_0(2, 1)$$

$$W = V + \begin{array}{c} \text{---} \\ \text{---} \end{array} V \chi_0 V + \begin{array}{c} \text{---} \\ \text{---} \end{array} V \chi_0 V \begin{array}{c} \text{---} \\ \text{---} \end{array} V \chi_0 V + \dots$$

GW in the RPA



RPA total energies (ACFDT)

The “RPA” total energy is given by:

$$E[n] = T_{KS}[\{\psi_i\}] + E_H[n] + E_X[\{\psi_i\}] + E_{\text{ion-el}}[n] + E_c$$

with the RPA correlation energy

$$E_c = \sum_{\mathbf{q}} \int_0^{\infty} \frac{d\omega}{2\pi} \text{Tr}\{\ln[1 - \chi_0(\mathbf{q}, i\omega)\nu] + \chi_0(\mathbf{q}, i\omega)\nu\}$$

and the Independent-Particle polarizability: $\chi^0(\mathbf{r}, \mathbf{r}', \omega) := \frac{\partial \rho_{\text{ind}}(\mathbf{r}, \omega)}{\partial v_{\text{eff}}(\mathbf{r}', \omega)}$

$$\begin{aligned} \chi_{\mathbf{G}, \mathbf{G}'}^0(\mathbf{q}, \omega) &= \frac{1}{\Omega} \sum_{nn' \mathbf{k}} 2w_{\mathbf{k}} (f_{n' \mathbf{k}+\mathbf{q}} - f_{n' \mathbf{k}}) \\ &\quad \times \frac{\langle \psi_{n' \mathbf{k}+\mathbf{q}} | e^{i(\mathbf{q}+\mathbf{G})\mathbf{r}} | \psi_{n \mathbf{k}} \rangle \langle \psi_{n \mathbf{k}} | e^{-i(\mathbf{q}+\mathbf{G}')\mathbf{r}'} | \psi_{n' \mathbf{k}+\mathbf{q}} \rangle}{\epsilon_{n' \mathbf{k}+\mathbf{q}} - \epsilon_{n \mathbf{k}} - \omega - i\eta} \end{aligned}$$

$\ln(1 - \chi_0 v) + \chi_0 v =$	$-\frac{\text{Tr}[\chi_0 v \chi_0 v]}{2}$	$-\frac{\text{Tr}[\chi_0 v \chi_0 v \chi_0 v]}{3}$	$-\frac{\text{Tr}[\chi_0 v \chi_0 v \chi_0 v \chi_0 v]}{4}$...
----------------------------------	---	--	---	-----

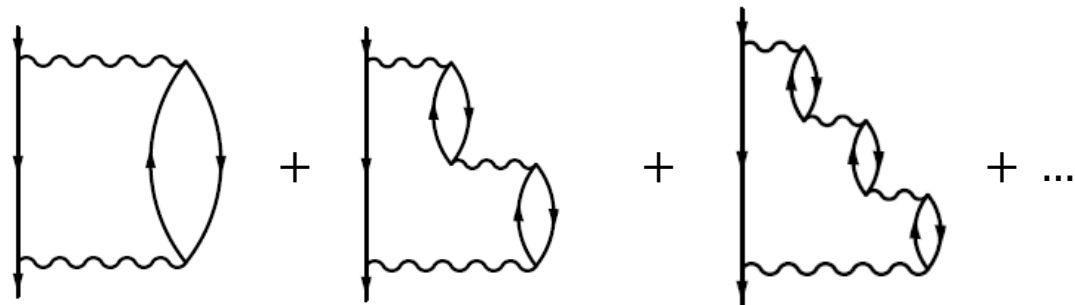
In terms of diagrams

$$\ln(1 - \chi_0 v) + \chi_0 v = -\frac{\text{Tr}[\chi_0 v \chi_0 v]}{2} - \frac{\text{Tr}[\chi_0 v \chi_0 v \chi_0 v \chi_0 v]}{3} - \frac{\text{Tr}[\chi_0 v \chi_0 v \chi_0 v \chi_0 v \chi_0 v]}{4} + \dots$$

2nd. order 3rd. order 4th. order

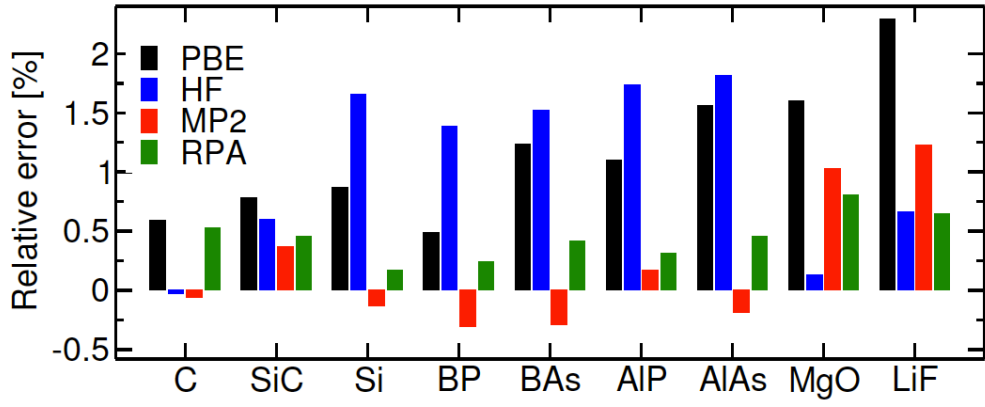
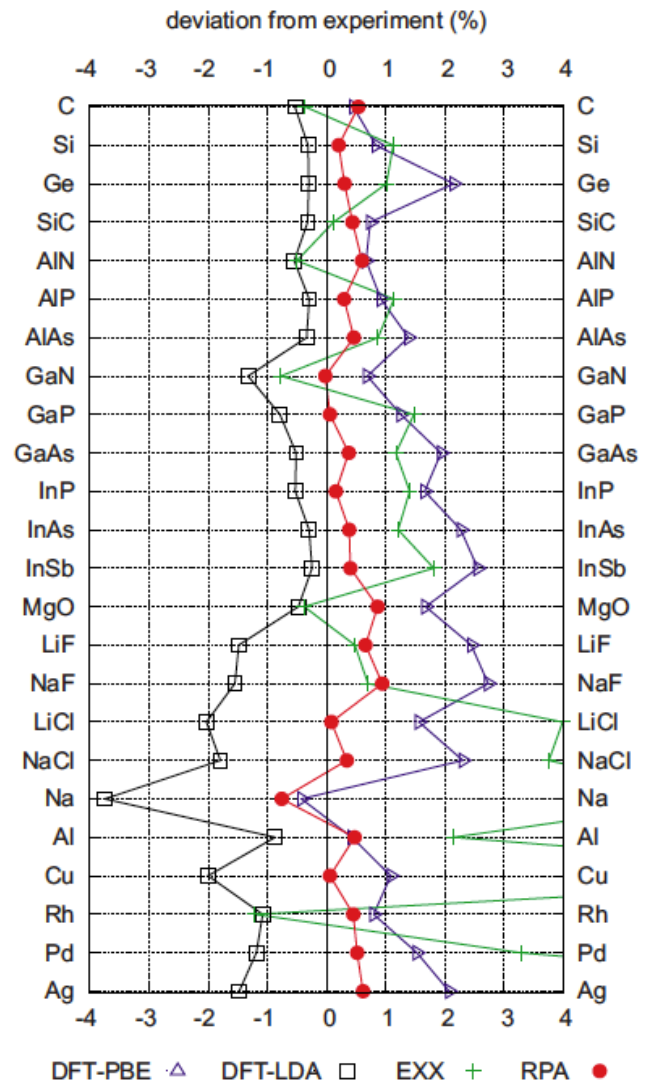
The derivate w.r.t. G
yields GW!

$$\frac{\partial E_c}{\partial G} = \Sigma$$



RPA: lattice constants

J. Harl et al., PRB 81, 115126 (2010)



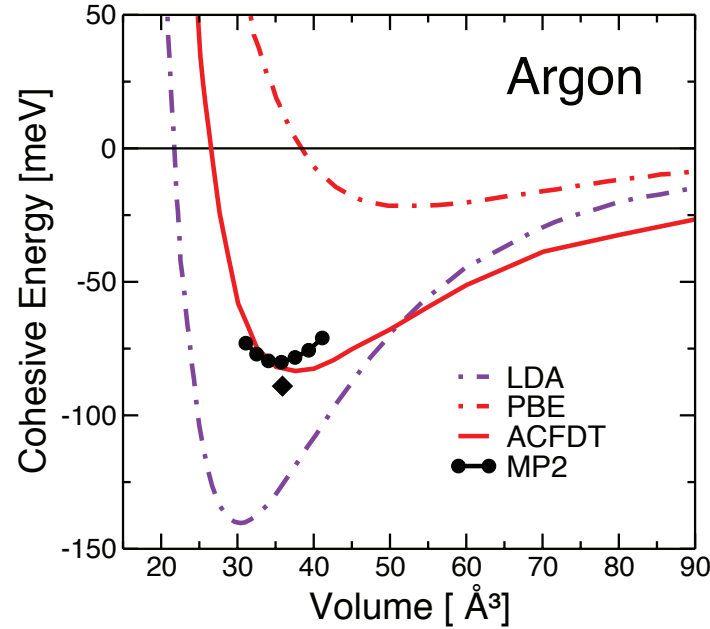
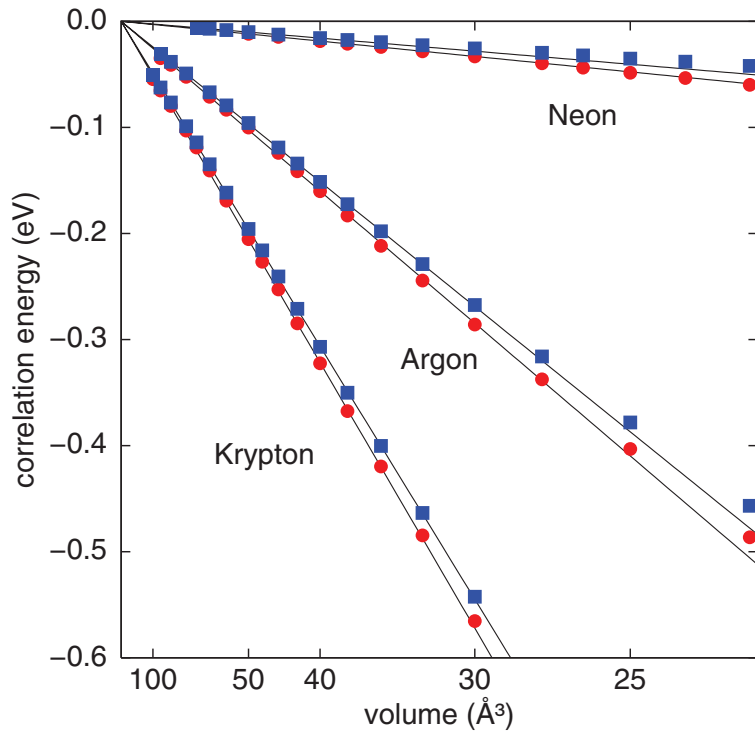
Deviations w.r.t. experiment
(corrected for zero-point vibrations)

	MRE	MARE
PBE	1.2	1.2
HF	1.1	1.1
MP2	0.2	0.4
RPA	0.5	0.4

(in %)

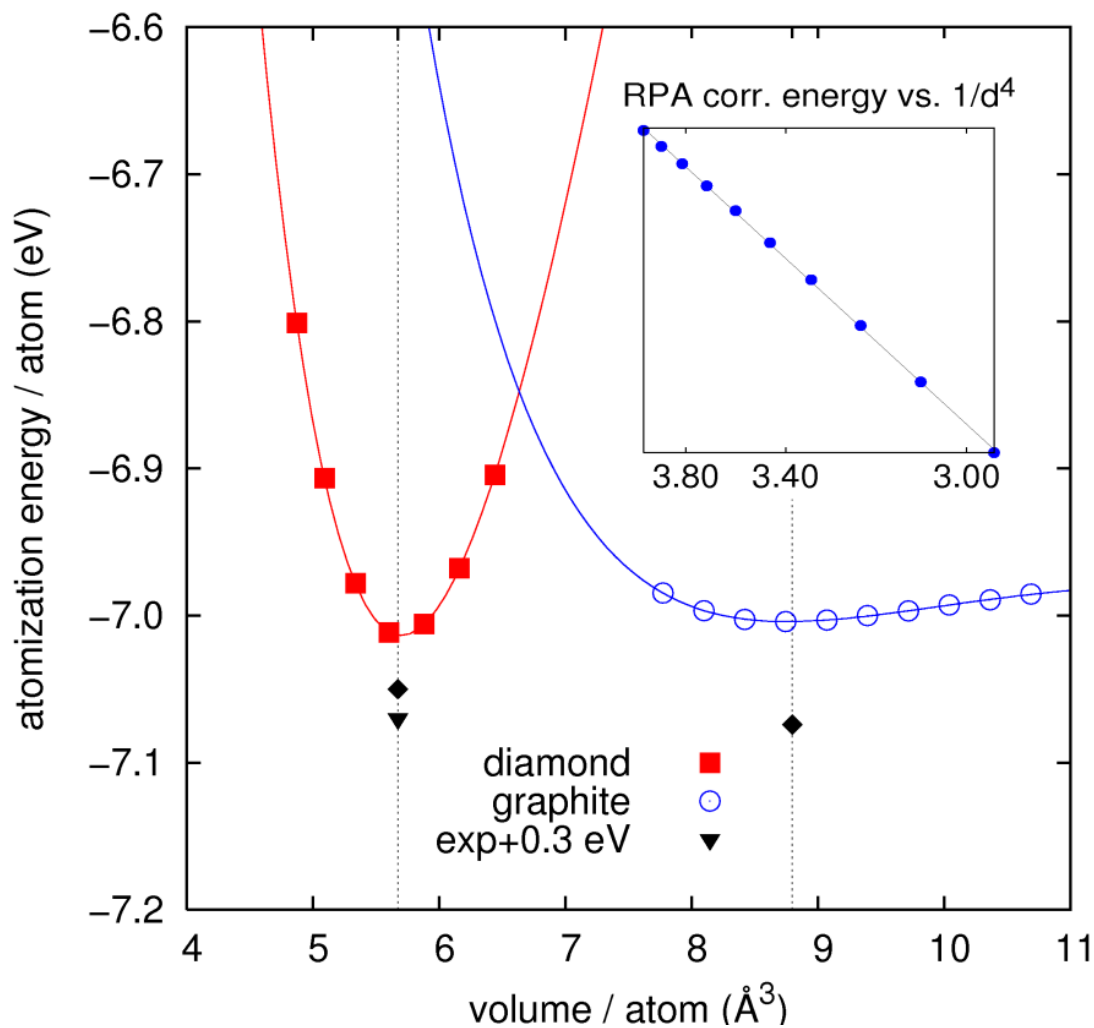
RPA: noble gas solids

J. Harl and G. Kresse, PRB 77, 045136 (2008)



	C_6 coefficients		
	RPA(LDA)	RPA(PBE)	Exp.
Ne	62	53	47
Ar	512	484	455
Kr	1030	980	895

Graphite vs. Diamond



$1/d^4$ behavior at short distances

	QMC (Galli)	RPA	EXP
$d(\text{\AA})$	3.426	3.34	3.34
C_{33}		36	36-40
E(meV)	56	48	43-50

J. Harl, G. Kresse,
PRL 103, 056401 (2009).
S. Lebeque, et al.,
PRL 105, 196401 (2010).

RPA: heats of formation

J. Harl and G. Kresse, PRL 103, 056401 (2009)

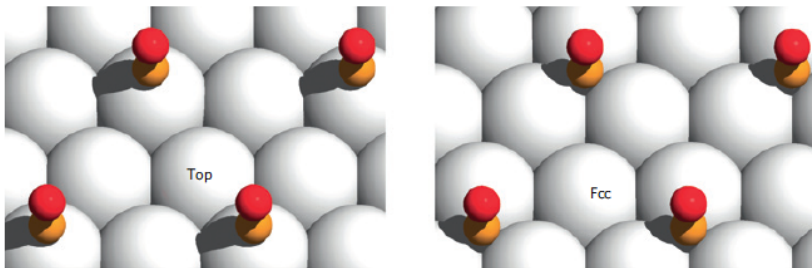
Heats of formation w.r.t. normal state at ambient conditions (in kJ/mol)



	PBE	Hartree-Fock	RPA	EXP
LiF	570	664	609	621
NaF	522	607	567	576
NaCl	355	433	405	413
MgO	516	587	577	603
MgH ₂	52	113	72	78
AlN	262	350	291	321
SiC	51	69	64	69

RPA: CO @ Pt(111) and Rh(111)

Schimka et al., Nature Materials 9, 741 (2010)



RPA:

- increases surface energy
and
- decreases adsorption energy

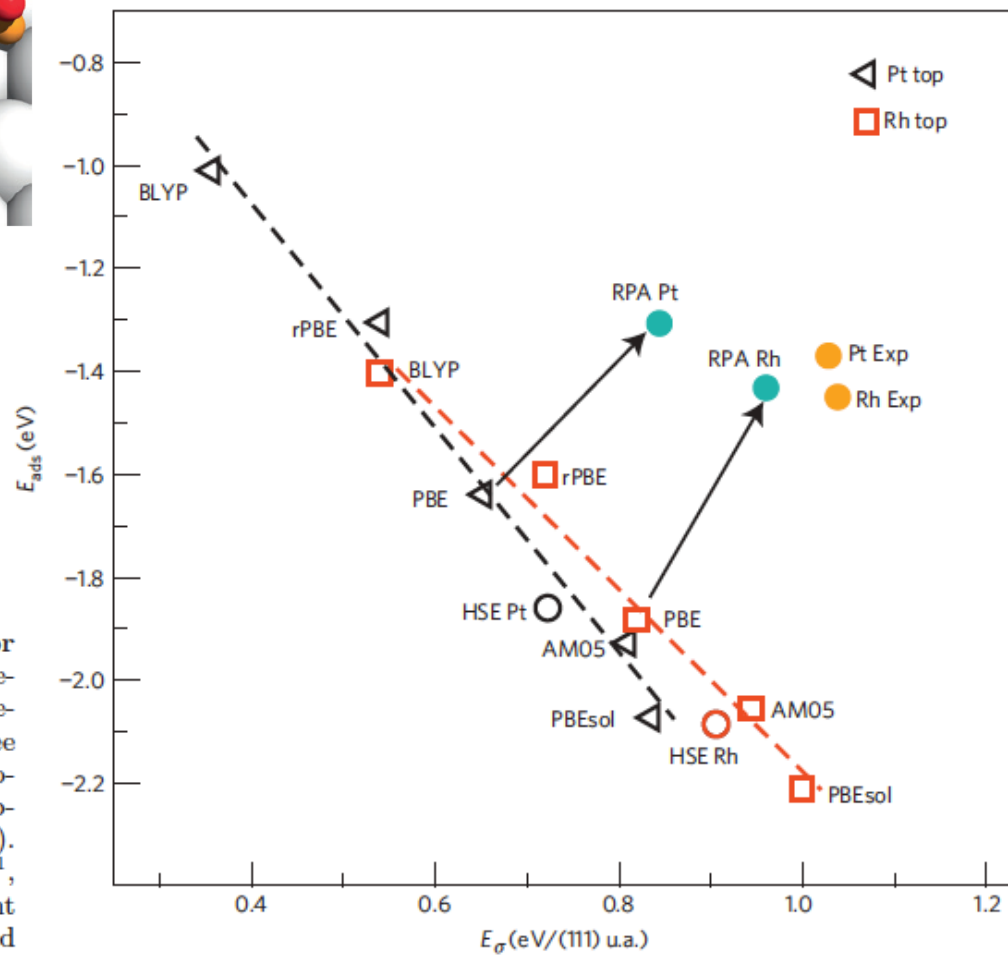


FIG. 1: Atop CO adsorption and surface energies for Pt(111) and Rh(111). (a) Considered CO adsorption geometries for a (2×2) surface cell. Semi-local functionals predict CO to adsorb in the fcc hollow site coordinated to three metal atoms on Pt and Rh, whereas experiments unequivocally show adsorption atop a metal atom. (b) Atop adsorption energies versus surface energies for Pt(111) and Rh(111). Various semi-local functionals were used: AM05¹⁰, PBEsol¹¹, PBE⁸, rPBE¹² and BLYP¹³, in order of increasing gradient corrections. Furthermore the hybrid functional HSE¹⁸ based on the PBE functional was used.

- DFT does well for the metallic surface, but not for the CO: $2\pi^*$ (LUMO) too close to the Fermi level.
- HSE does well for the CO, but not for the surface: d -metal bandwidth too large.
- GW gives a good description of both the metallic surface as well as of the CO $2\pi^*$ (LUMO). The CO 5σ and 1π are slightly underbound.

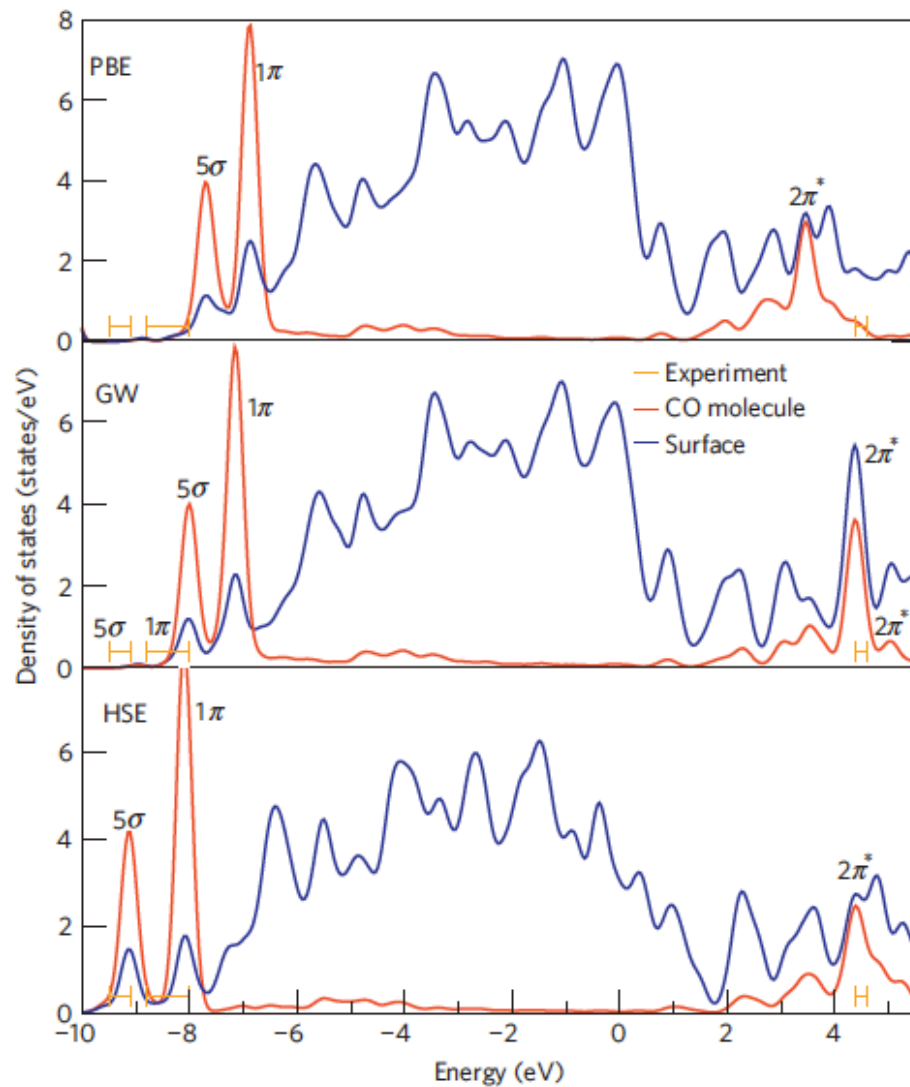


Figure 2 | Electronic DOS for CO adsorbed atop a Pt atom on Pt(111). The DOS is evaluated using DFT (PBE), the RPA (GW) and a hybrid functional (HSE). Experimental photoemission data for the $2\pi^*$ state are from ref. 19, for the 5σ and 1π state from ref. 20.

RPA:

- Right site preference
- Good adsorption energies
- Excellent lattice constants
- Good surface energies

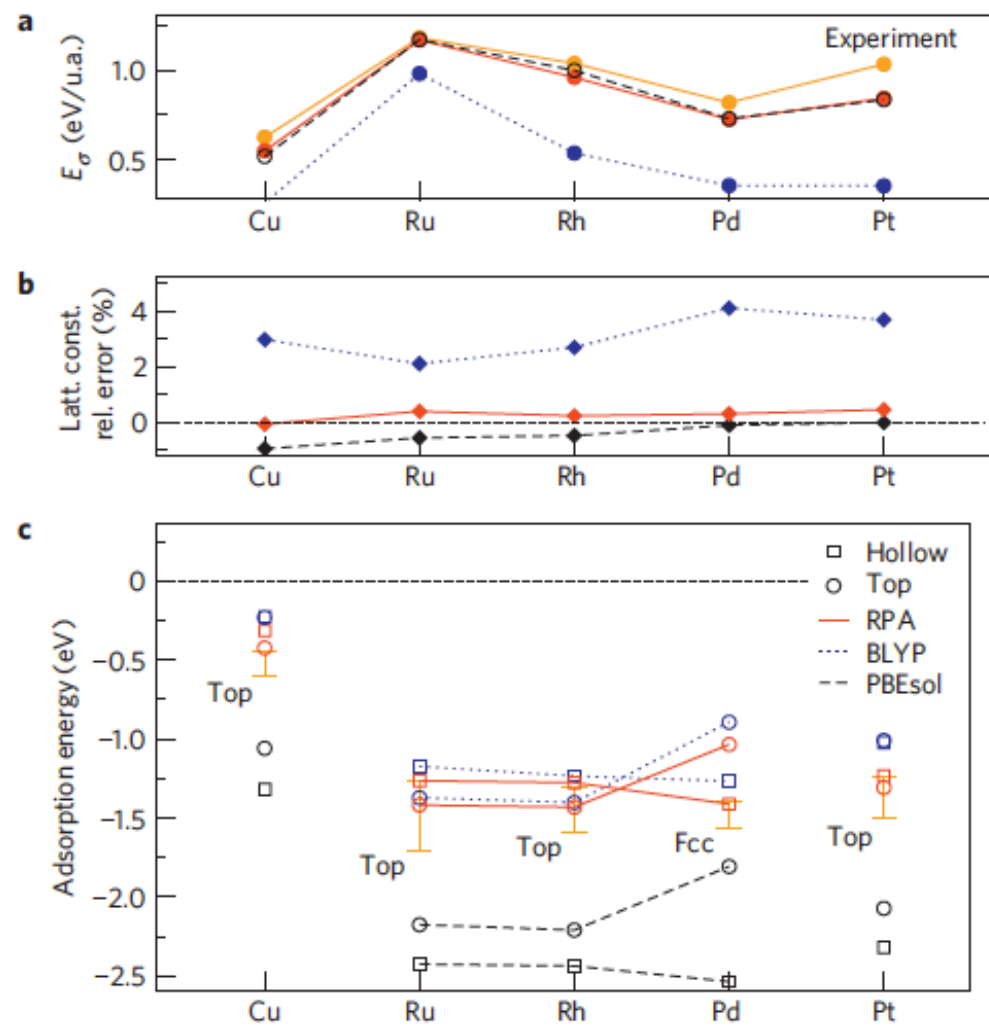


Figure 3 | Surface energies, lattice constants and adsorption energies. a, FCC(111) surface energies (E_σ) for PBEsol, BLYP and RPA. Experimental surface energies are deduced from liquid-metal data^{24,25}. b, Lattice constants for PBEsol, RPA and BLYP. c, Adsorption energies for the atop and hollow sites of CO on Cu, late 4d metals and Pt for PBEsol, RPA and BLYP. Experimental data with error bars are from ref. 26. The error bars correspond to the spread of the experimental results.

Cubic scaling RPA

As shown by Adler and Wiser, the IP polarizability χ^0 can be straightforwardly calculated from $\{\psi, \epsilon\}$:

$$\begin{aligned}\chi_{\mathbf{G}, \mathbf{G}'}^0(\mathbf{q}, \omega) = & \frac{1}{\Omega} \sum_{nn'k} 2w_k (f_{n'k+q} - f_{nk}) \\ & \times \frac{\langle \psi_{n'k+q} | e^{i(\mathbf{q}+\mathbf{G})\mathbf{r}} | \psi_{nk} \rangle \langle \psi_{nk} | e^{-i(\mathbf{q}+\mathbf{G}')\mathbf{r}'} | \psi_{n'k+q} \rangle}{\epsilon_{n'k+q} - \epsilon_{nk} - \omega - i\eta}\end{aligned}$$

Expensive: this scales as N^4 !

Cubic-scaling RPA

M. Kaltak, J. Klimeš, and G. Kresse, PRB 90, 054115 (2014)

Evaluate the Green's function in “imaginary” time:

$$G(\mathbf{r}, \mathbf{r}', i\tau) = \sum_n \psi_n(\mathbf{r}) \psi_n^*(\mathbf{r}') e^{-\epsilon_n \tau}$$

and the polarizability as:

$$\chi^0(\mathbf{r}, \mathbf{r}', i\tau) = -G(\mathbf{r}, \mathbf{r}', i\tau)G(\mathbf{r}, \mathbf{r}', -i\tau)$$

Followed by a cosine-transform:

$$\chi^0(\mathbf{r}, \mathbf{r}', i\tau) \xrightarrow{\text{CT}} \chi^0(\mathbf{r}, \mathbf{r}', i\omega)$$

Now the worst scaling steps are the evaluation of the Greens function (N^3), and

$$E_c = \int_0^\infty \frac{d\omega}{2\pi} \text{Tr}\{\ln[1 - \chi_0(i\omega)\nu] + \chi_0(i\omega)\nu\}$$

(which scales as N^3 due to the diagonalization involved in evaluating the “ \ln ”).

The evaluation of the polarizability scales quadratically (N^2)!

But storing G and χ is expensive! → we need small sets of cleverly chosen “ τ ” and “ ω ”

The “minimax” fit

Express a function $f(x)$ in a basis of N functions $\{\varphi(\alpha_i, x) | i = 1, \dots, N\}$, such that the error:

$$\eta(\vec{\alpha}, \vec{\beta}, x) = f(x) - \sum_i \beta_i \varphi(\alpha_i, x)$$

is “as small as possible”.

Choose $\{(\alpha_i, \beta_i) | i = 1, \dots, N\}$ so that the *maximum error*:

$$\|\eta\|_\infty := \max_{a \leq x \leq b} |\eta(\vec{\alpha}, \vec{\beta}, x)|$$

is minimized.

This solution, $\{(\alpha_i^*, \beta_i^*) | i = 1, \dots, N\}$, is the so-called “minimax” solution

The “minimax” frequency grid

M. Kaltak, J. Klimeš, and G. Kresse, JCTC 10, 2498 (2014)

The IP polarizability can be written as (Adler&Wiser):

$$\chi(i\omega) = \sum_{\mu} \chi_{\mu} \phi(\omega, x_{\mu}) \quad \begin{aligned} \chi_{\mu}(=ia) &= \langle i|\mathbf{r}|a\rangle\langle a|\mathbf{r}'|i\rangle \\ x_{\mu}(=ia) &= \epsilon_a - \epsilon_i \end{aligned}$$

where $\phi(\omega, x) = \frac{2x}{x^2 + \omega^2}$

Determine a frequency grid and quadrature weights by expressing the “2nd-order direct Møller-Plesset energy”

$$E_c^{(2)} = -\frac{1}{8\pi} \int_{-\infty}^{\infty} d\omega \{\chi(i\omega)\nu\}^2$$

in the basis $\{\phi(\omega_i, x)|i = 1, \dots, N\}$ in the minimax sense:

$$\{(\gamma_k^*, \omega_k^*)|k = 1, \dots, N\} \quad \eta(\vec{\gamma}, \vec{\omega}, x) = \frac{1}{x} - \frac{1}{\pi} \sum_{k=1}^N \gamma_k \phi^2(\omega_k, x) \quad E_g \leq x \leq \max(\epsilon_a - \epsilon_i)$$

$$E_c^{(2)} = -\frac{1}{8\pi} \int_{-\infty}^{\infty} d\omega \{\chi(i\omega)\nu\}^2 \longrightarrow E_c^{(2)} \approx -\frac{1}{8\pi} \sum_{k=1}^N \gamma_k^* \{\chi(i\omega_k^*)\nu\}^2$$

The “minimax” time grid

M. Kaltak, J. Klimeš, and G. Kresse, JCTC 10, 2498 (2014)

Alternatively the IP polarizability can be written as:

$$\hat{\chi}(i\tau) = \sum_{\mu} \chi_{\mu} \hat{\phi}(\tau, x_{\mu}) \quad \begin{aligned} \chi_{\mu}(=ia) &= \langle i|\mathbf{r}|a\rangle\langle a|\mathbf{r}'|i\rangle \\ x_{\mu}(=ia) &= \epsilon_a - \epsilon_i \end{aligned}$$

where $\hat{\phi}(\tau, x) = e^{-x|\tau|}$

Determine a frequency grid and quadrature weights by expressing the “2nd-order direct Møller-Plesset energy”

$$E_c^{(2)} = -\frac{1}{4} \int_{-\infty}^{\infty} d\tau \{\hat{\chi}(i\tau)\nu\}^2$$

in the basis $\{\hat{\phi}(\tau_i, x)|i = 1, \dots, N\}$ in the minimax sense:

$$\{(\sigma_k^*, \tau_k^*)|k = 1, \dots, N\} \quad \hat{\eta}(\vec{\sigma}, \vec{\tau}, x) = \frac{1}{2x} - \sum_{k=1}^N \sigma_k \hat{\phi}^2(\tau_k, x) \quad E_g \leq x \leq \max(\epsilon_a - \epsilon_i)$$

$$E_c^{(2)} = -\frac{1}{4} \int_{-\infty}^{\infty} d\tau \{\hat{\chi}(i\tau)\nu\}^2 \quad \longrightarrow \quad E_c^{(2)} \approx -\frac{1}{4} \sum_{k=1}^N \sigma_k^* \{\hat{\chi}(i\tau_k^*)\nu\}^2$$

The non-uniform cosine transform

M. Kaltak, J. Klimeš, and G. Kresse, JCTC 10, 2498 (2014)

The cosine transform of $\chi(i\omega) \leftrightarrow \chi(i\tau)$:

$$\chi(i\omega) = 2 \int_0^\infty d\tau \hat{\chi}(i\tau) \cos(\omega\tau) \quad \hat{\chi}(i\tau) = \frac{1}{\pi} \int_0^\infty d\omega \chi(i\omega) \cos(\omega\tau)$$

is reformulated on the minimax frequency and time grids as

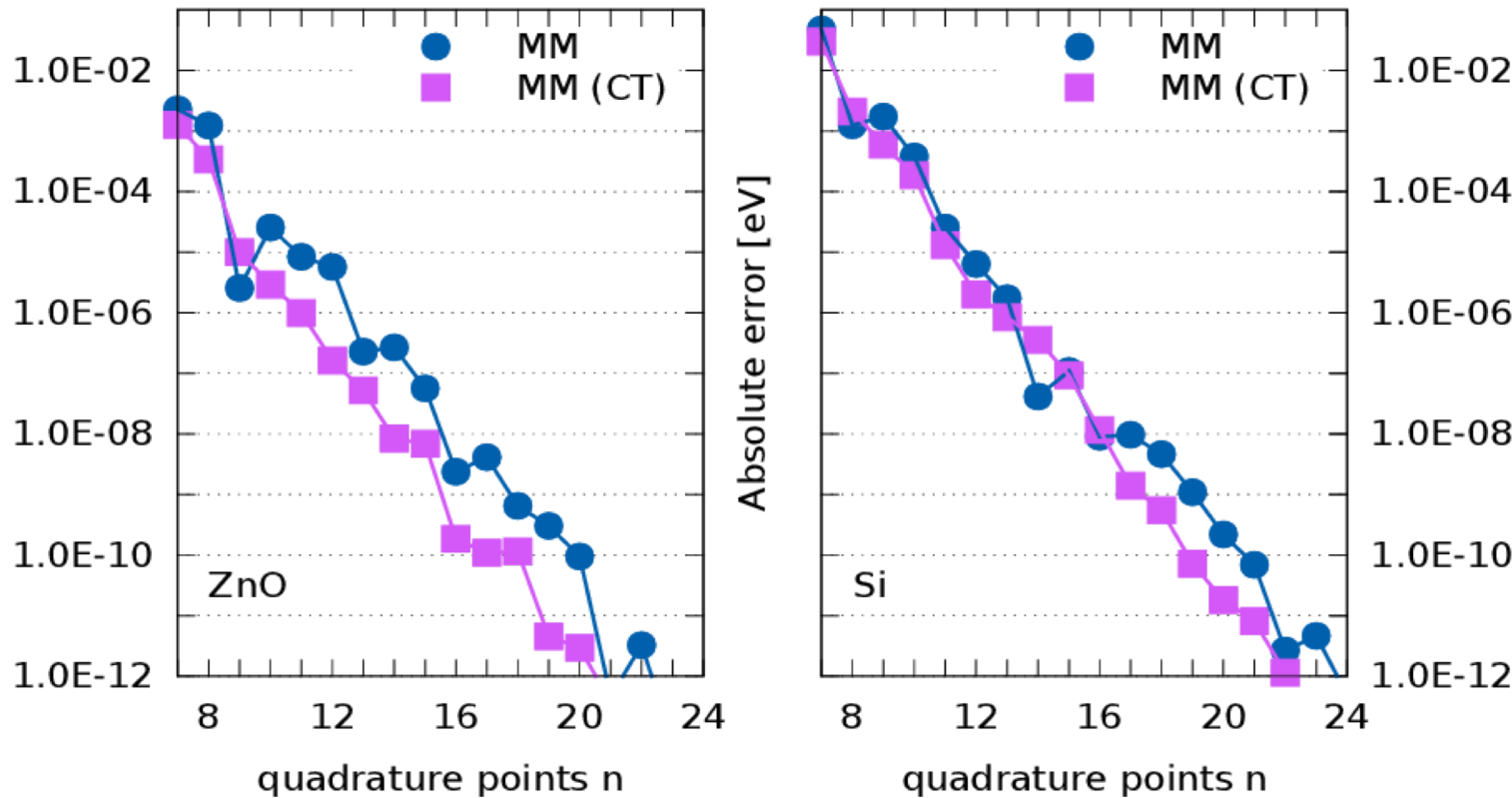
$$\chi(i\omega_k) = \sum_{l=1}^N a_{kl} \hat{\chi}(i\tau_l) \quad a_{kl} = w_{kl} \cos(\omega_k^* \tau_l^*)$$

where the coefficients w_{kl} are the minimax solution to the following fitting problem:

$$\eta^c(\vec{w}_k, x) = \phi(\omega_k^*, x) - \sum_{l=1}^N w_{kl} \cos(\omega_k^* \tau_l^*) \hat{\phi}(\tau_l^*, x) \xrightarrow{\text{minimax fit}} \{w_{kl}^* | k, l = 1, \dots, N\}$$

for fixed $\{\omega_k^*\}$ and $\{\tau_k^*\}$, and for $E_g \leq x \leq \max(\epsilon_a - \epsilon_i)$.

How good are the grids: ZnO and Si



- N^4 RPA calculations entirely in frequency
- N^2 calculation of polarizability in time, then transformation to frequency
(200 atoms on 200 cores in about one hour)

M. Kaltak, J. Klimeš, and G. Kresse, JCTC 10, 2498 (2014); PRB 90, 054115 (2014).

Scaling

New RPA code (VASP6):

- Scales linearly in the number of k-points (as DFT), instead of quadratically as for conventional RPA and hybrid functionals
- Scales cubically in system size (as DFT).

Prefactors are much larger than in DFT, but calculations for 200 atoms take less than 1 hour (128 cores)

Si defect calculations: 64-216 atoms

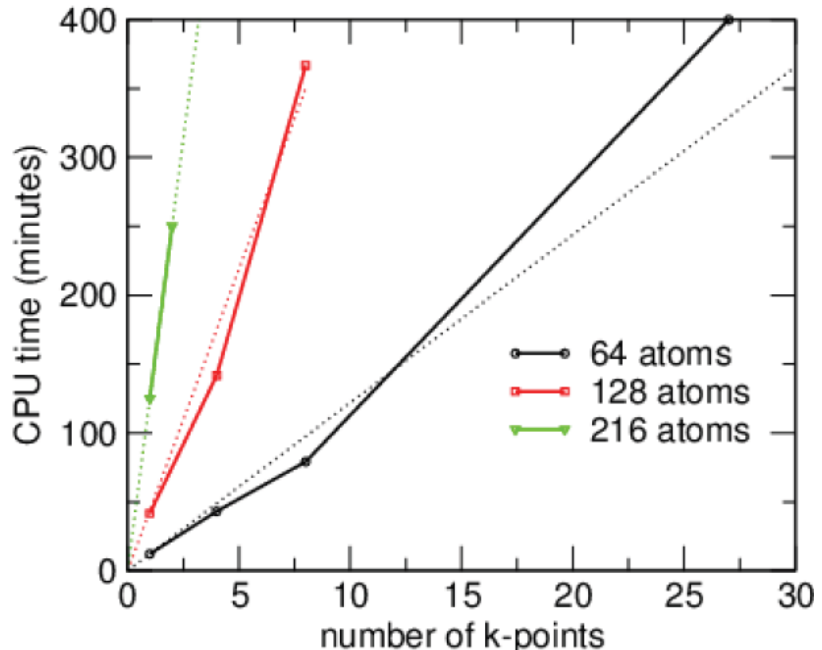
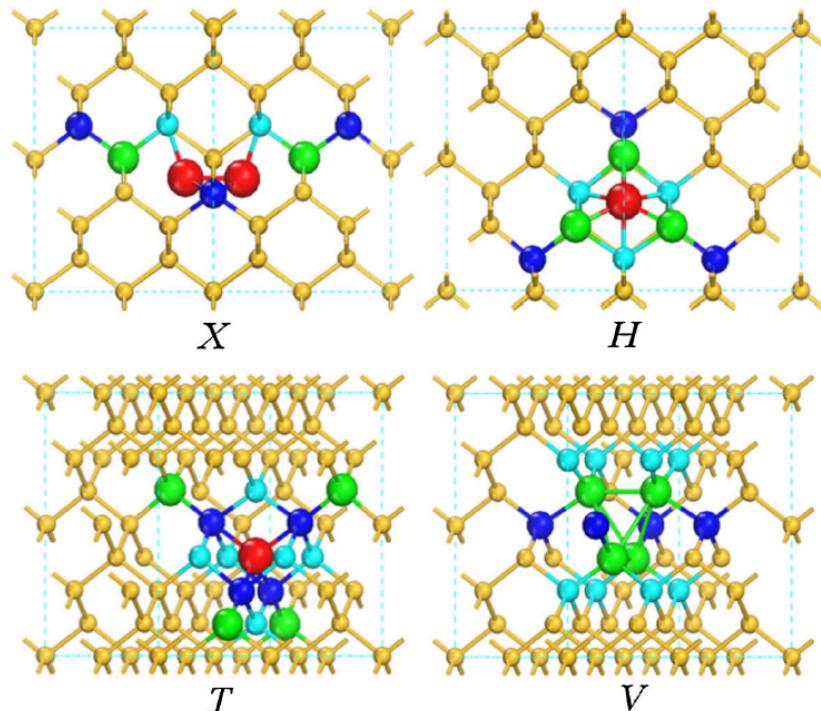


TABLE I. Timings in minutes for an RPA calculation for different bulk Si bcc cells. The calculations are done for the Γ point only and the number of cores is increased with system size. Since one of the computational steps scales only quadratically with system size, the total scaling is better than cubic.

Atoms	Cores	Time	Time \times cores/atoms ³ $\times 10^3$
54	32	14.3	2.91
128	64	83.2	2.54
250	128	299.9	2.45

Defect formation energies in Si

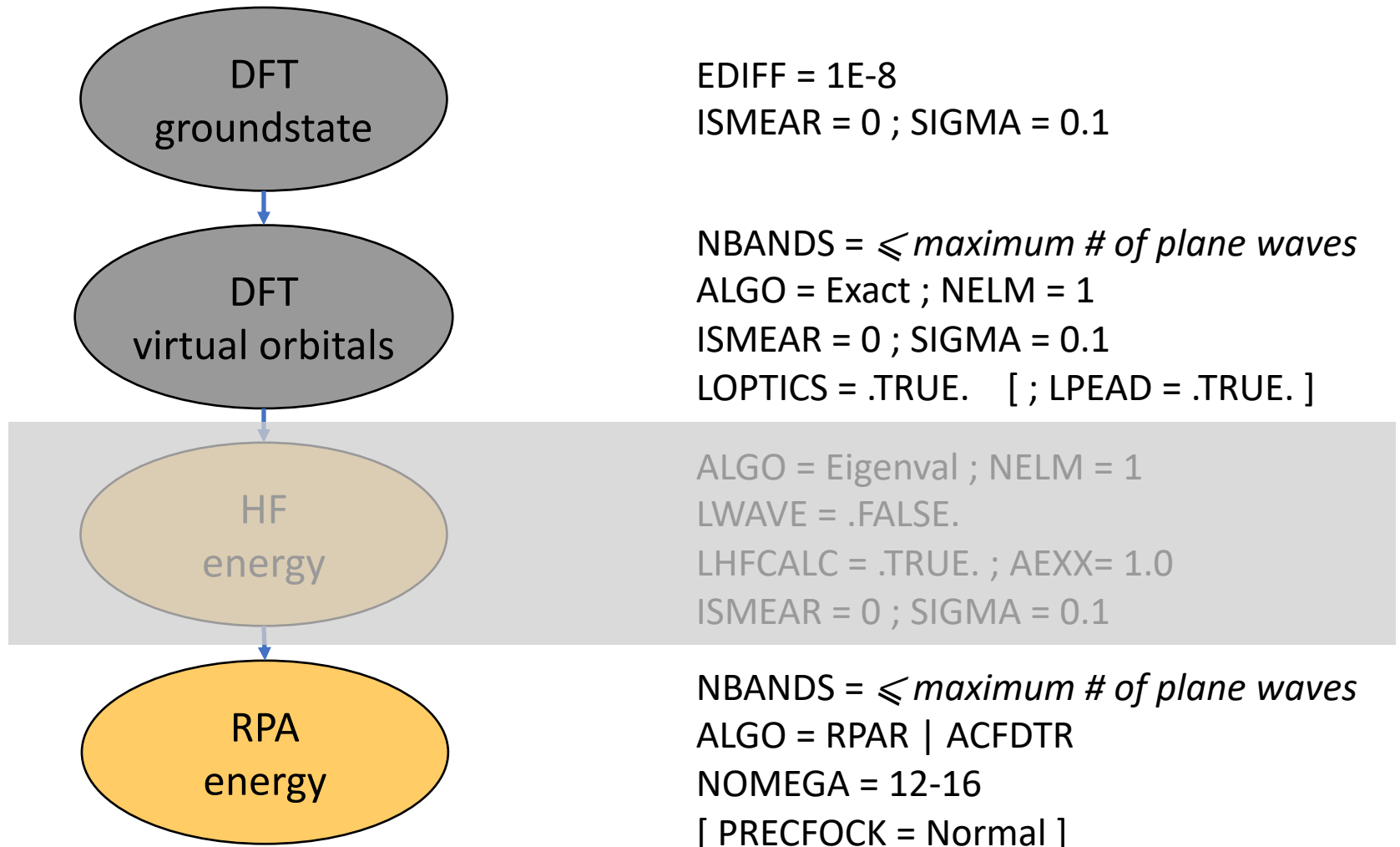
	PBE	HSE	HSE(+vdW)	QMC	RPA
Dumbbell X	3.56	4.43	4.41	4.4(1)	4.28
Hollow H	3.62	4.49	4.40	4.7(1)	4.44
Tetragonal T	3.79	4.74	4.51	5.1(1)	4.93
Vacancy	3.65	4.19	4.38		4.40



pictures and HSE+vdW:
Gao and Tkatchenko,
PRL 111, 045501 (2013).

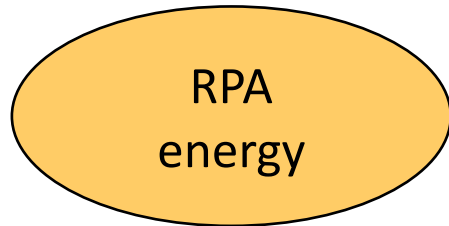
QMC:
Parker, Wilkins, and Hennig,
Phys. Status Solidi B 248, 267 (2011).

RPA total energy calculation: flow chart



... or all in one go!

When one does **not** specify NBANDS, VASP will run all consecutive steps in one go:



EDIFF = 1E-8
ISMEAR = 0 ; SIGMA = 0.1
LOPTICS = .TRUE. ; LPEAD = .TRUE.

ALGO = RPAR | ACFDTR
NOMEGA = 12-16

[PRECFOCK = Normal]

[NBANDSEXACT = # of bands in G]

In this case the number of bands used to compute the Greens function is specified by means of the NBANDSEXACT tag (optional).

An example: SiC

INCAR:

```
ALGO = ACFDTR
NOMEGA = 16
NBANDSEXACT = 120
PRECFOCK = NORMAL

LOPTICS = .TRUE. ; LPEAD = .TRUE.

ISMEAR = 0 ; SIGMA = 0.05
EDIFF = 1E-8

LWAVE = .FALSE.
```

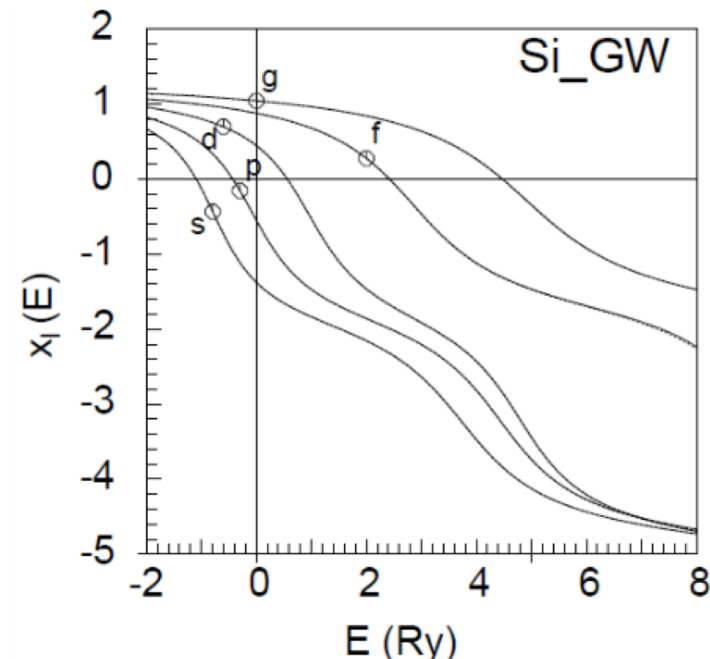
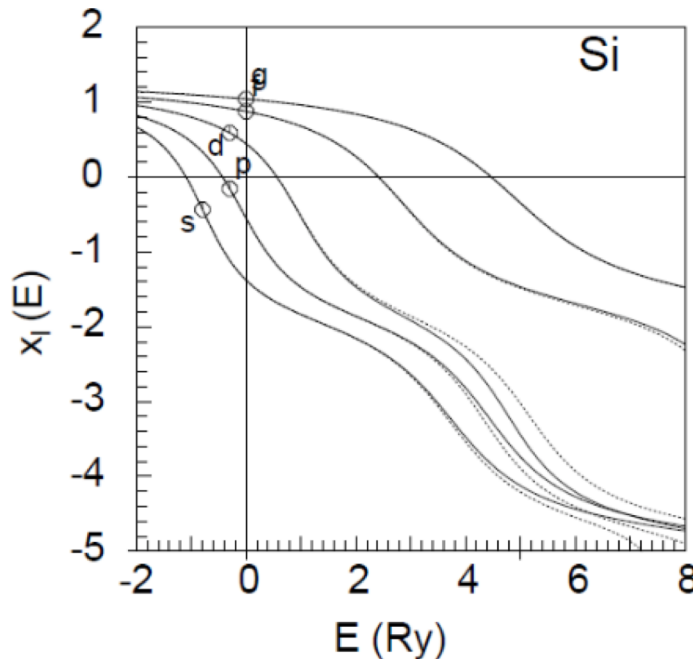
KPOINTS:

```
Automatically generated mesh
0
Gamma
3 3 3
0 0 0
```

POSCAR:

```
SiC
4.35
0.5 0.5 0.0
0.0 0.5 0.5
0.5 0.0 0.5
1 1
cart
0.00 0.00 0.00
0.25 0.25 0.25
```

The GW potentials: *_GW POTCAR files



H	0,0
Li	Be
0,1	0,5
Na	Mg
0,4	0,0
K	Ca
0,1	0,4
Rb	Sr
0,1	0,2
Cs	Ba
0,1	0,3

$$\Delta(\text{PAW})_{(\text{VASP})} = 0.4 \text{ meV/atom}$$

He	0,0
B	0,2
Al	0,3
In	0,2
Ga	0,8
Ge	0,7
C	0,2
Si	0,1
Sn	0,8
As	0,8
N	0,7
P	0,0
Sb	0,5
Se	0,4
O	0,1
S	0,2
Te	0,5
F	0,1
Cl	0,0
Br	0,2
Kr	0,1
Ne	0,1

stdout

```
running    8 mpi-ranks, with    1 threads/rank
distrk: each k-point on    8 cores,    1 groups
distr: one band on    1 cores,    8 groups
using from now: INCAR
vasp.6.1.2 22Jul20 (build Jul 22 2020 23:58:52) complex
```

```
POSCAR found : 2 types and      2 ions
scalAPACK will be used
LDA part: xc-table for Pade appr. of Perdew
POSCAR, INCAR and KPOINTS ok, starting setup
FFT: planning ...
WAVECAR not read
```

	N	E	dE	d eps	ncg	rms	rms(c)
DAV:	1	-0.807695689957E+00	-0.80770E+00	-0.25358E+03	80	0.517E+02	
DAV:	2	-0.160589369121E+02	-0.15251E+02	-0.12187E+02	80	0.986E+01	
DAV:	3	-0.166458202722E+02	-0.58688E+00	-0.58688E+00	96	0.179E+01	
DAV:	4	-0.166475623089E+02	-0.17420E-02	-0.17420E-02	64	0.947E-01	
DAV:	5	-0.166475838631E+02	-0.21554E-04	-0.21554E-04	104	0.120E-01	0.992E+00
DAV:	6	-0.146217932388E+02	0.20258E+01	-0.80384E+00	96	0.241E+01	0.883E+00
DAV:	7	-0.145343752600E+02	0.87418E-01	-0.37382E-01	88	0.483E+00	0.577E+00
DAV:	8	-0.145238445286E+02	0.10531E-01	-0.25946E-02	80	0.163E+00	0.429E-01
DAV:	9	-0.145238173443E+02	0.27184E-04	-0.60800E-04	96	0.212E-01	0.972E-02
DAV:	10	-0.145240248823E+02	-0.20754E-03	-0.27113E-04	88	0.148E-01	0.118E-02
DAV:	11	-0.145240278179E+02	-0.29356E-05	-0.22309E-05	96	0.467E-02	0.104E-02
DAV:	12	-0.145240279045E+02	-0.86635E-07	-0.18940E-06	80	0.143E-02	0.134E-03
DAV:	13	-0.145240279035E+02	0.10211E-08	-0.32364E-08	88	0.170E-03	

“DFT groundstate calculation”

```
The Fermi energy was updated, please check that it is located mid-gap
values below the HOMO (VB) or above the LUMO (CB) will cause erroneous energies
E-fermi : 9.6656
optical routines
imaginary and real dielectric function
direction      1
direction      2
direction      3
```

“Exact diagonalization and LOPTICS step”

stdout (cont.): set up “minimax” grids

```
responsefunction array rank=      120
NTAUPAR set to  8 based on available memory per rank (MAXMEM=   2710 MB)

set NWRITE>2 for more details about minimax calculation
number of imaginary grid points requested:      16
number of distinct grids requested:  4
quadrature errors minimized for energies in [ 0.250E+01, 0.186E+03 ]
time grid (T=0) determined with error: 0.6315E-12
fermionic grid (T=0, re) determined with error: 0.1995E-11
bosonic grid (T=0, re) determined with error: 0.1995E-11
fermionic grid (T=0, im) determined with error: 0.2003E-11
bosonic grid (re): 0.1995E-11
  0.3979      1.2370      2.2122      3.4344      5.0481
  7.2506     10.3202     14.6578     20.8519     29.7850
 42.8243     62.2141     92.0388    141.1698    235.3471
 502.7281

fermionic grid (re): 0.1995E-11
  0.3979      1.2370      2.2122      3.4344      5.0481
  7.2506     10.3202     14.6578     20.8519     29.7850
 42.8243     62.2141     92.0388    141.1698    235.3471
 502.7281

fermionic grid (im): 0.2003E-11
  0.8065      1.7011      2.7842      4.1811      6.0600
  8.6543     12.2972     17.4731     24.9000     35.6703
 51.5185     75.4212    113.2309    179.3773    325.9188
 1022.1852

time grid: 0.6315E-12
  0.0009      0.0048      0.0121      0.0234      0.0398
  0.0628      0.0950      0.1402      0.2039      0.2934
  0.4195      0.5973      0.8486      1.2074      1.7333
  2.5647
```

NTAUPAR is set automatically based on the available memory: either set manually by means of the MAXMEM-tag, or read from /proc/meminfo (MemAvailable)

“frequency”

“time”

stdout (cont.): distribution over ω and τ

```
Distributing 16 bosonic points into 8 group(s)
Group: 1 has 1 cores and 2 bosonic point(s)
Group: 2 has 1 cores and 2 bosonic point(s)
Group: 3 has 1 cores and 2 bosonic point(s)
Group: 4 has 1 cores and 2 bosonic point(s)
Group: 5 has 1 cores and 2 bosonic point(s)
Group: 6 has 1 cores and 2 bosonic point(s)
Group: 7 has 1 cores and 2 bosonic point(s)
Group: 8 has 1 cores and 2 bosonic point(s)
```

(Here running on 8 MPI-ranks)

NOMEGAPAR = 8

```
Distributing 16 fermionic points into 8 group(s)
Group: 1 has 1 cores and 2 fermionic point(s)
Group: 2 has 1 cores and 2 fermionic point(s)
Group: 3 has 1 cores and 2 fermionic point(s)
Group: 4 has 1 cores and 2 fermionic point(s)
Group: 5 has 1 cores and 2 fermionic point(s)
Group: 6 has 1 cores and 2 fermionic point(s)
Group: 7 has 1 cores and 2 fermionic point(s)
Group: 8 has 1 cores and 2 fermionic point(s)
```

```
Distributing 16 time points into 8 group(s)
Group: 1 has 1 cores and 2 time point(s)
Group: 2 has 1 cores and 2 time point(s)
Group: 3 has 1 cores and 2 time point(s)
Group: 4 has 1 cores and 2 time point(s)
Group: 5 has 1 cores and 2 time point(s)
Group: 6 has 1 cores and 2 time point(s)
Group: 7 has 1 cores and 2 time point(s)
Group: 8 has 1 cores and 2 time point(s)
```

NTAUPAR = 8

min. memory requirement per mpi rank 448.9 MB, per node 3591.2 MB

Performance-wise it is optimal to have NTAUPAR = NOMEGAPAR = NOMEWA.
Prerequisite: there has to be enough memory for NTAUPAR = NOMEWA,
and the number of MPI-ranks must be a multiple of NOMEWA.

OUTCAR: plane wave basis set limit

ENCUTGW (= 2/3 ENCUT)

ENCUTGWSOFT (= 0.8 ENCUTGW)

cutoff energy	smooth cutoff	RPA	correlation	Hartree contr. to MP2
182.607	146.086	-11.6224735165	-18.3767216933	
173.912	139.129	-11.5729431431	-18.3208811769	
165.630	132.504	-11.5167771988	-18.2570942952	
157.743	126.194	-11.4562166727	-18.1878044293	
150.232	120.185	-11.3922444110	-18.1141897888	
143.078	114.462	-11.3188094759	-18.0290907645	
136.264	109.012	-11.2261996896	-17.9208940815	
129.776	103.821	-11.1299318178	-17.8073101088	
linear regression converged value		-12.3629185205		-19.2342034424

“Extrapolated to infinite basis set limit”: $E_c(G) = E_c(\infty) + \frac{A}{G^3}$

Convergence tests:

- Investigate convergence w.r.t. ENCUT (not ENCUTGW or ENCUTGWSOFT).
- If possible converge energy differences not absolute correlation energies.

OUTCAR: RPA total energy

HF energy using frozen KS orbitals

Free energy of the ion-electron system (eV)

```
-----  
alpha Z      PSCENC =      10.57645478  
Ewald energy TEWEN =     -285.31033112  
-Hartree energ DENC =     -32.94127495  
-exchange EXHF =        74.67798493  
-V(xc)+E(xc) XCENC =    0.00000000  
PAW double counting = 1473.50548166 -1473.60386908  
entropy T*S EENTRO =   -0.00000000  
eigenvalues EBANDS =   -21.25334570  
atomic energy EATOM =   229.23716772
```

```
-----  
HF-free energy TOTEN = -25.11173175 eV  
exchange ACFDT corr. = -0.00000000 see jH, gK, PRB 81, 115126  
HF+correlation energy = -36.73420527  
HF+E_corr(extrapolated)= -37.47465027
```

diagrammatic approximations of correlation energy (eV)

```
-----  
direct MP2      EDMP2 =      -19.23420344  
random phase     ERPA =      -12.36291852  
GW Galitskii-Migdal EGWGM =  0.00000000
```

Without extrapolation

“Extrapolated to infinite
basis set limit”

RPA: important INCAR tags

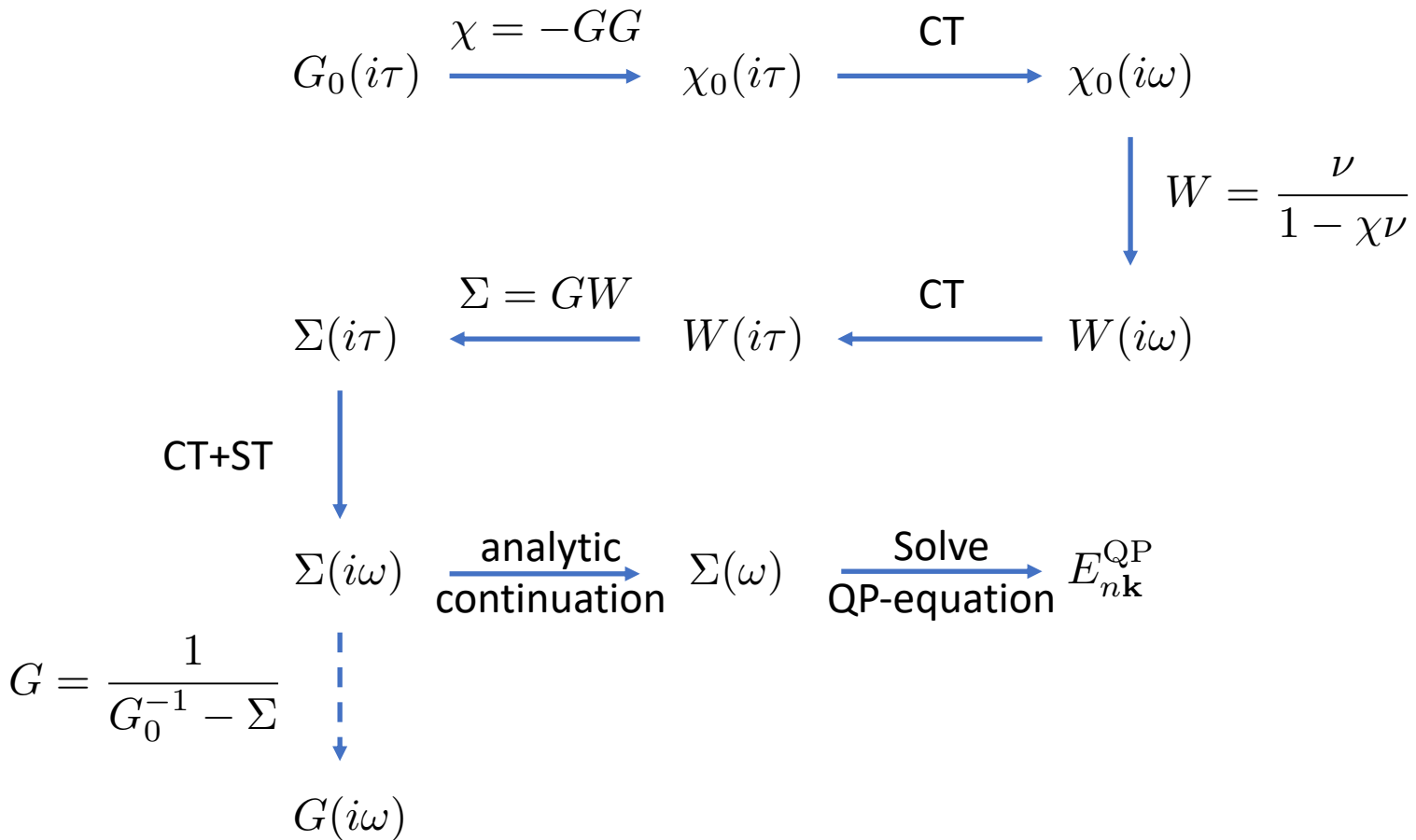
- ALGO
- NOMEGA
- PRECFOCK
- NTAUPAR
- NOMEgapar
- MAXMEM
- NBANDS
- NBANDSEXACT
- ENCUTGW

Visit our [WIKI!](#)

Especially the parts on:
[Cubic scaling RPA calculations](#)

Cubic-Scaling GW

P. Liu, M. Kaltak, J. Klimeš, and G. Kresse, PRB 94, 165109 (2016)



- Minimax grids:
M. Kaltak, J. Klimeš, and G. Kresse, JCTC 10, 2498 (2014); PRB 90, 054115 (2014).
- Cubic-scaling RPA total energies (ACFDT):
M. Kaltak, J. Klimeš, and G. Kresse, PRB 90, 054115 (2014).
- Cubic-scaling RPA quasi-particles (GW):
P. Liu, M. Kaltak, J. Klimeš, and G. Kresse, PRB 94, 15109 (2016).
- Finite temperature grids (!):
M. Kaltak and G. Kresse, PRB 101, 205145 (2020)



Dr. Merzuk Kaltak
(VASP Software GmbH)

Forces in the RPA

$$\frac{\partial E}{\partial R} = \langle \psi | \frac{\partial H}{\partial R} | \psi \rangle + \langle \frac{\partial \psi}{\partial R} | H | \psi \rangle + \langle \psi | H | \frac{\partial \psi}{\partial R} \rangle$$

Non-Hellmann-Feynman!

Hellmann-Feynman theorem: when the orbitals are eigenstates of the Hamiltonian, the second and third terms on the RHS are zero.

In the RPA we need to consider "non-Hellmann-Feynman" contributions!

These take the following form:

"from linear response"

$$\langle \frac{\partial \psi}{\partial R} | H | \psi \rangle + \langle \psi | H | \frac{\partial \psi}{\partial R} \rangle \rightarrow \left(\int G_0(i\omega) \left. \frac{\partial E_{\text{RPA}}}{\partial G} \right|_{i\omega} G_0(i\omega) d\omega \right) \frac{\partial V_{\text{KS}}}{\partial R}$$

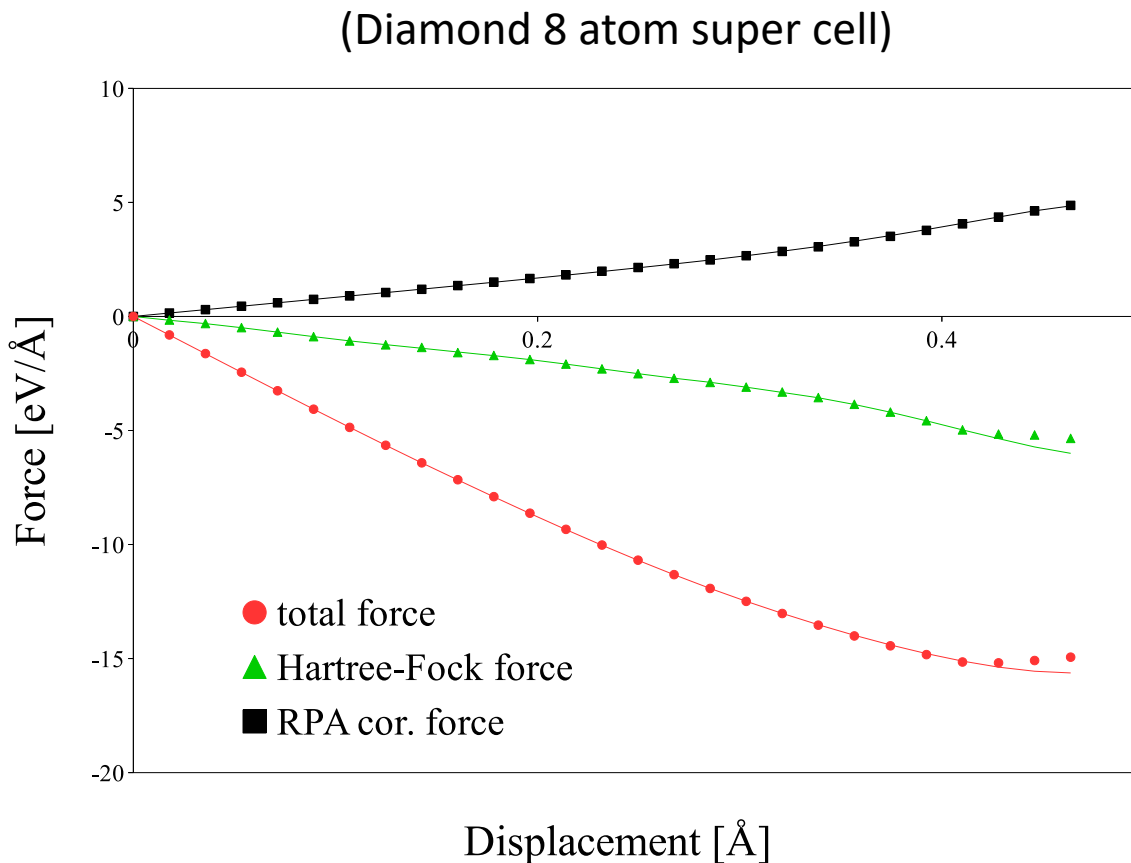
$$\frac{\partial E_H}{\partial G} = V_H$$

$$\frac{\partial E_X}{\partial G} = V_X$$

$$\frac{\partial E_c}{\partial G} = \Sigma$$

Forces in the RPA

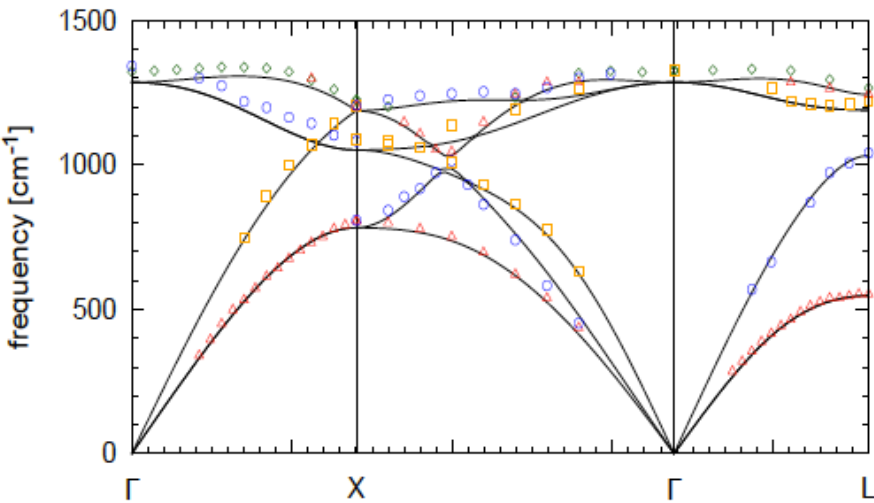
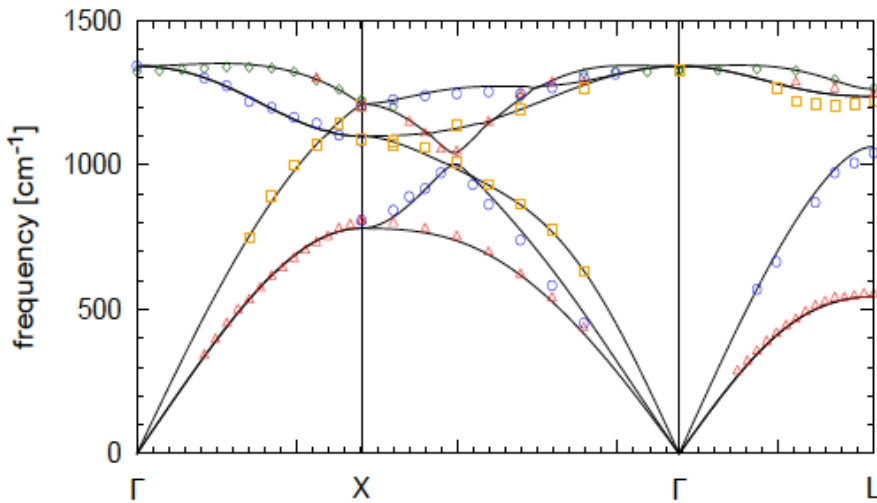
A test: "RPA forces" (lines) vs. energy derivatives from finite differences (symbols):



RPA

Diamond (128 atom super cell)

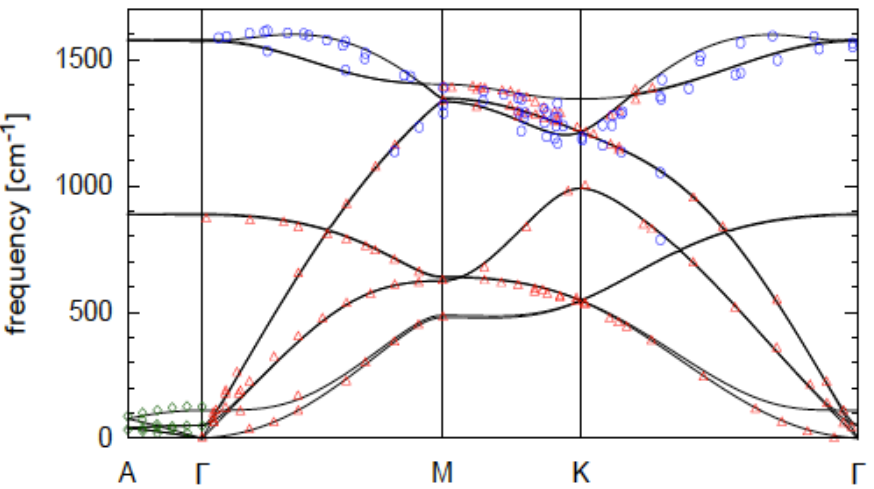
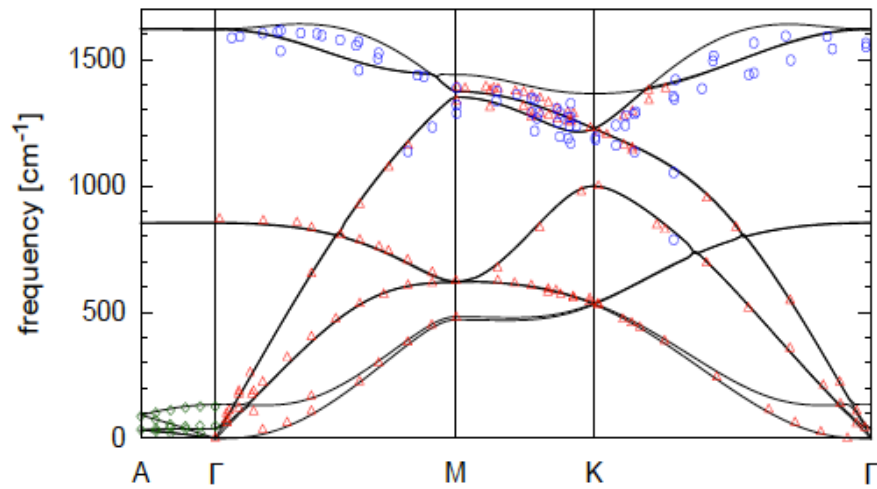
PBE



RPA

Graphite (128 atom super cell)

PBE



Summary

- Beyond DFT: the RPA
 - Well balanced description of all bond types (metallic, covalent, ionic, vdW)
 - Unfortunately energy differences can still not be predicted with chemical accuracy
 - But at the moment the optimal balance between accuracy and computational effort
- Cubic-Scaling RPA
 - Both for total energies as well as for quasi-particles
 - Minimax frequency and time grids
 - Near future: finite temperature RPA
- Forces in the RPA

The End

Thank you for your attention!